Ophthalmic Research

Ophthalmic Res , DOI: 10.1159/000549368
Received: August 7, 2025
Accepted: October 25, 2025
Published online: November 7, 2025

Bisretinoids as a Source of Early Photoreceptor Pathology in Stargardt Disease

Mata NL, Weng S, Michaelides M, Charbel Issa P, Quinodoz M, Rivolta C, Scholl HPN

ISSN: 0030-3747 (Print), eISSN: 1423-0259 (Online)
https://www.karger.com/ORE
Ophthalmic Research

Bisretinoids as a Source of Early Photoreceptor Pathology in Stargardt Disease

Nathan L. Mata[a], Stephanie Weng[b], Michel Michaelides[c], Peter Charbel Issa[d], Mathieu Quinodoz[e,f,g], Carlo Rivolta[e,f,g], Hendrik P.N. Scholl[a,h,i,j]

[a] Belite Bio, Inc, San Diego, California, USA
[b] SWeng Solutions LLC, San Francisco, California, USA
[c] UCL Institute of Ophthalmology, University College London, and Moorfields Eye Hospital, London, United Kingdom
[d] Dept. of Ophthalmology, Technical University of Munich, Munich, Germany
[e] Ophthalmic Genetics Group, Institute of Molecular and Clinical Ophthalmology Basel (IOB), Basel, Switzerland
[f] Department of Ophthalmology, University of Basel, Basel, Switzerland
[g] Department of Genetics and Genome Biology, University of Leicester, Leicester, UK
[h] Medical University of Vienna, Department of Clinical Pharmacology, Vienna, Austria
[i] Pallas Kliniken AG, Pallas Klinik Zürich, Zürich, Switzerland
[j] European Vision Institute, Basel, Switzerland

Short Title: Bisretinoids and Retinal Pathology in STGD1

Corresponding Author:
Nathan L. Mata
E-mail address: nmata@belitebio.com

Keywords: bisretinoids, fundus autofluorescence, lipofuscin, retinal pigment epithelium, Stargardt disease

Abstract

Background: Stargardt disease (STGD1) due to bi-allelic mutations in the *ABCA4* gene is the most frequent single-gene retinal disease with a genetic prevalence of about 1 in 7,000. Pathology in STGD1 is due to dysfunction of a retina-specific vitamin A transporter which causes accumulation of cytotoxic vitamin A byproducts known as *bisretinoids*. Bisretinoids produce a distinct autofluorescent emission within affected cells that is seen to precede atrophy of the retinal pigment epithelium (RPE), photoreceptor cell death, and vision loss. This sequence of pathogenesis, and the fact that formation and accumulation of bisretinoids begins within photoreceptors, suggests early pathology may occur within photoreceptor cells. Here, relevant literature is reviewed to explore the relationship between bisretinoids, fundus autofluorescence, and photoreceptor function/integrity in STGD1 with a focus on early-stage disease and potential biomarkers for clinical investigation.

Summary: Currently accepted primary endpoints in STGD1 clinical trials include quantification of areas where the autofluorescence signal is lacking due to the death of RPE and photoreceptor cells. Importantly, many patients with early-stage STGD1 cannot be monitored in this way as they present clinically prior to RPE or photoreceptor loss at a pre-atrophic stage and without significant visual impairment. Imaging analyses of patients with early-stage disease have shown increased fundus autofluorescence and compromised photoreceptor integrity and/or visual function deficits in the absence of atrophic retinal lesions. These findings implicate early accumulation of bisretinoid toxins within the retina as an underlying causative factor and provide an impetus to determine the relevance of these measures as surrogate endpoints or biomarkers for disease progression in STGD1 clinical trials.

Key Messages: Early recognition and treatment of patients with STGD1 who have relatively healthy retinal tissue will likely yield a more favorable visual prognosis. Accordingly, there is a need to identify early disease initiators and progression patterns. The reviewed data support the hypothesis that bisretinoid accumulation within photoreceptors may be responsible for the observed early retinal pathology and vision loss. Clinical evaluation of therapeutics intended to reduce bisretinoid accumulation in early-stage STGD1 patients will likely provide a greater understanding of the role of bisretinoids in disease progression and potential for vision preservation.

Introduction

Stargardt disease (STGD1, OMIM# 248200) is a progressive retinal degenerative disease, which is typically detected in childhood or early adulthood, varies in severity, and sometimes may not be diagnosed until later in adulthood [1,2]. Patients with childhood-onset STGD1 tend to develop early visual acuity (VA) loss, compromised photoreceptor function on electroretinography (ERG), and rapid enlargement of RPE atrophy [3-5]. In contrast, patients with adult-onset STGD1 show milder retinal dysfunction at diagnosis and a much slower loss of VA [6-8]. The observed phenotypic differences between patients with childhood- versus adult-onset STGD1 are believed to be due to more deleterious genetic variants in the childhood-onset population [5,7].

Inheritance of STGD1 occurs in an autosomal recessive manner and is due to disease-causing variants in the ATP binding cassette A4 gene (*ABCA*4) which codes for the retina-specific ATP-binding cassette transporter, ABCR [9]. The ABCR protein resides at the margins of rod and cone photoreceptor discs where it plays a critical role in vitamin A recycling by removing all-*trans* retinal from photoreceptors [10]. Free all-*trans* retinal has been shown to be extremely cytotoxic [11] and perhaps explains why the ABCR protein has evolved in mammalian vision. Dysfunction of ABCR leads to the formation and accumulation of cytotoxic vitamin A byproducts (bisretinoids) which produce a distinct autofluorescence emission due to their retinoid composition.

Severity of *ABCA4*-related retinopathy and its phenotypic presentation may vary considerably, explaining why historically, different terms were used for the different clinical presentations (e.g. Stargardt disease, fundus flavimaculatus, cone-rod dystrophy). Unifying features across all phenotypes of *ABCA4*-related retinopathy are the most pronounced disease manifestation in the macula and—at least in most cases—the increased accumulation of bisretinoids and lipofuscin in the retinal pigment epithelium (RPE) before it degenerates [12,13].

Bisretinoids are initially formed within photoreceptor cells and are continually taken into the underlying RPE, where they are processed into stable cytotoxic compounds with altered autofluorescence properties. The unique autofluorescence associated with bisretinoids within photoreceptors, compared with RPE [14], provides an opportunity to examine pathology caused by these different bisretinoid species, particularly in early-stage disease prior to the onset of RPE atrophy. In fact, visual loss which precedes ophthalmoscopic abnormalities in childhood-onset STGD1 [5] could be explained by bisretinoid toxicity within photoreceptors [15].

The majority of published clinical findings in STGD1 relate to clinical features of patients examined in adulthood. While these studies have advanced our understanding of underlying disease mechanisms, natural history, and outcome metrics for clinical trials, far less is known about pathology and disease progression in early-stage disease. The rapid deterioration of VA in childhood-onset STGD1 highlights the importance of early intervention in this patient population and the need to identify the underlying cause(s). Based upon the sequence of pathology in STGD1, bisretinoid formation within photoreceptors is the earliest pathological feature and may likely be the cause of, or contribute to, VA loss prior to excessive lipofuscin accumulation and RPE atrophy in many cases of early-onset STGD1. The various clinical studies described below provide evidence of early-stage cellular and functional changes that are associated with increased autofluorescence (i.e., bisretinoid accumulation) and could be useful as biomarkers and/or surrogate endpoints in future clinical trials.

Prevalence of STGD1

The prevalence of STGD1 is often reported to be 1 in 8,000 to 1 in 10,000. Although, population-specific prevalence data for STGD1 are not readily available, the advent of genomic databases now allows the estimation of genetic prevalence (i.e., the proportion of individuals in the population who are expected to be affected due to their genotype, based on the frequency of unaffected carriers of pathogenic *ABCA4* variants in the general population). For instance, Hanany et al. calculated such prevalence to be as high as 1 in 2,740 in individuals of European descent [16], a figure that is in line with epidemiological data obtained by Xiao and Lauschke on sequencing information from 141,456

individuals across seven ethnogeographic groups, estimating the global prevalence of STGD1 as 4.3 per 10,000 individuals [17].

The following explanations or a combination thereof may explain the difference between these calculations and previous estimates: (1) Undiagnosed disease—patients may remain undiagnosed, especially those with late-onset disease without significant symptoms due to foveal sparing and hence well-preserved VA; such phenotype may occur particularly in patients carrying one hypomorphic *ABCA*4 variant in combination with a more severe variant; (2) Incorrect diagnosis—patients may be diagnosed with a clinically similar but pathogenetically different disease. For instance, late-onset *ABCA4*-related retinal disease may be incorrectly classified as the more common age-related macular degeneration, and other monogenetic disease may be suspected in younger patients (e.g., if characteristic signs such as flecks are not obviously present); (3) Genetic modifiers—some individuals with biallelic *ABCA4* mutations and additional protective genetic modifiers might remain without clinically significant disease expression. Candidate modifier genes would for instance be those coding for enzymes of the visual cycle or those influencing melanin biosynthesis or degradation. As an example, in the *Abca4*$^{-/-}$ STGD1 mouse model, polymorphisms in *RPE65* on an albino background may modify the severity of the retinal phenotype [18,19]. These genetic modifiers could also modify the penetrance of some variants. For example, the frequent variant p.Asn1868Ile, associated with a late-onset form of STGD1 was shown to have a penetrance below 5% [20]; (4) Environmental modifiers—disease manifestation in the *Abca4*$^{-/-}$ mouse may depend on the amount of vitamin A intake [21], indicating that modifiable environmental factors might also have an impact on the "detected prevalence" of *ABCA4*-related retinopathy.

The translation of carrier frequencies into disease prevalence depends on how variants with low clinical penetrance are taken into account. Therefore, for the computation of the prevalence of classic STGD1 or the late-onset form, the sums of allele frequency computed by Cornelis et al. [22] was used. This data was derived from 5,579 patients with STGD1 and comprised 1,619 unique variants computed for the 7 different ethnicities from the Genome Aggregation Database (gnomAD). For classic STGD1 prevalence, the sum of combinations for severe/severe severe/moderate, moderate/moderate and severe/mild with complete penetrance was determined. For the late-onset form associated with p.Asn1868Ile (N1868I), the number of patients with severe/N1868I is multiplied by 5% to account for the reduced penetrance of this frequent hypomorphic variant. Table 1 and Figure 1 show the estimated prevalence for various world populations. There is significant heterogeneity in prevalence, with higher prevalence in the African population due to a specific missense variant, p.Arg2107His that has a frequency of 2.1% in people of African ethnicity from gnomAD. This was also found recently by Xiao et al. [17].

Table 2 shows the estimated number of patients in some of the larger world geographies. For the United States, the breakdown of genetic populations is shown in Table 3 and allows estimation of the number of affected patients to be between 47,000 and 59,000. For both Europe and China, the estimated affected patient number is likely larger than 100,000.

The Origin of Bisretinoids in STGD1

Under normal physiological conditions, all-*trans* retinal released from photoactivated rhodopsin rapidly and reversibly reacts with phosphatidylethanolamine (PE) to form *N*-retinylidene-phosphatidylethanolamine (*N*-ret-PE). The ABCR protein binds *N*-ret-PE and acts as a 'flippase' to translocate *N*-ret-PE from inside of the photoreceptor disc to the cytoplasmic surface allowing enzymatic reduction of all-*trans* retinal to all-*trans* retinol and re-entry into the RPE for recycling [10]. Dysfunction of the ABCR protein, as in STGD1, leads to excessive accumulation of all-*trans* retinal and *N*-ret-PE within photoreceptor disc membranes. The reactivity of *N*-ret-PE promotes a spontaneous condensation with a second molecule of retinal resulting in the accelerated formation of bisretinoid compounds—dihydro-*N*-retinylidene-*N*-retinyl-phosphatidylethanolamine (A2PE-H2) and its oxidized form (A2PE) which are the major bisretinoid species found in the retina [23-25].

Over the course of STGD1 disease progression, A2PE-H2 and A2PE are continually taken into the RPE through the normal diurnal phagocytic uptake of shed photoreceptor outer segment discs [26]. The bisretinoid-laden cellular debris is directed to the acidic environment of phagolysosomes where digestive enzymes cleave the PE moiety from the phosphatidyl-pyridinium structure producing a highly stable pyridinium bisretinoid compound known as *N*-retinylidene-*N*-retinylidene ethanolamine (A2E). Thus, A2PE-H2 and A2PE are precursors of A2E [24,27]. Once formed, A2E and its photo-oxidized forms, resist further degradation and accumulate within RPE phagolysosomes where they initiate a myriad of cytotoxic events including impaired phagolysosomal activity [28], induction of inflammation [29], activation of complement [30] and pro-angiogenic factors [31], accelerated cell damage in blue light [32], and generalized apoptotic cell death [33]. The dysfunction occurring within phagolysosomes compromises digestion of shed photoreceptor outer segment discs leading to accelerated accumulation of lipofuscin and compromised cellular function. Notably, the fluorescence emission spectrum from human RPE lipofuscin is consistent with the emission spectrum obtained from A2E [34].

Pathology in STGD1

Clinically, areas of excessive lipofuscin are observed on fundus autofluorescence (FAF) imaging as hyperautofluorescent yellowish deposits known as “flecks” in the posterior pole around the macula [35,36]. Because the hyperautofluorescence of flecks corresponds with the autofluorescent properties of A2E and related bisretinoids, fleck hyperautofluorescence has been attributed to a high bisretinoid content [37-39]. With disease progression, the initially well-defined flecks appear to migrate outward from the central macula in a centrifugal pattern. In late stages, flecks fade, leaving poorly demarcated hypoautofluorescent lesions consistent with RPE atrophy and photoreceptor cell loss [40,38]. The structural basis and location of flecks are poorly understood, and these lesions are assumed to be positioned at or just above the level of RPE [41-43]. Although, histological analyses of post-mortem STGD1 eyes have shown excessive accumulation of lipofuscin in both RPE cells and photoreceptor inner segments [44,33].

Based on the observed course of disease, it has been generally accepted that retinal pathology in STGD1 begins with the accumulation of A2E and related bisretinoids within the RPE, which compromise phagolysosomal activity leading to excessive lipofuscin accumulation followed by atrophy of the RPE [45]. Death of RPE cells then leads to loss of overlying photoreceptors and compromised visual function due to loss of trophic influences provided by the RPE [46]. While this scenario is consistent with anatomical observations, the potential cytotoxicity due to the accumulation of A2E precursors within photoreceptor cells has not been fully addressed.

Clinical evidence reveals a correspondence between early appearing autofluorescent lesions and subsequent loss of photoreceptor function or integrity, which either precedes or occurs in the absence of RPE atrophy, indicating that STGD1 may be a disease of the outer neural retina, with the RPE affected secondarily [38,39,47,48]. Findings from these studies will be discussed in a subsequent section of this review.

Learnings From Animal Models

The Abca4 Null Mutant Mouse Model

Much of our current understanding of the biology of disease in STGD1 has come from studies of mouse models. The first STGD1 model generated was an *Abcr* null (*Abca*4$^{-/-}$) mutant [23]. Phenotypic features of *Abca*4$^{-/-}$ mice included: (1) delayed rod dark adaptation; (2) transient accumulation of all-*trans*-retinal; (3) increase of PE in outer segments; (4) the presence of distinct bisretinoid species in the retina and RPE; and (5) dramatically increased lipofuscin in RPE cells.

One of the early studies of *Abca*4$^{-/-}$ mice aimed to determine the relationship between the bisretinoid fluorophores identified in the retina and RPE [27]. In this study, fluorescence emission spectra were obtained from flat-mounted samples of RPE–choroid and retina dissected from the eyeglobes of 8-month-old *Abca*4$^{-/-}$ mice. The emission spectrum from RPE-choroid tissue was maximal at ~550 nm, consistent with A2E (shown in Fig. 2, panel A, dashed line spectrum). In

contrast, the fluorescence emission spectrum from retina samples was maximal at ~625 nm and exhibited a considerably lower fluorescence emission intensity (shown in Fig. 2, panel A, solid line spectrum). Further analysis of the fluorophore observed in retina showed an age-dependent increase in fluorescence intensity (shown in Fig. 2, panel B) demonstrating a progressive accumulation of this autofluorescent species.

The identity of the fluorophore(s) observed in *Abca4*$^{-/-}$ retinas was confirmed following chromatographic analysis of the retinoids extracted from the retina explants. The chromatographic data revealed two major absorbing species (shown in Fig. 3, panel A, dashed line). The early eluting peak at ~6 minutes showed a spectrum that was similar to that of a retinoid-derived species; however, this compound showed no fluorescence emission (shown in Fig. 3, panel A, solid line) and was not studied further. In contrast, the peak eluting at ~26 minutes showed an absorbance spectrum that was consistent with a bisretinoid species, and a red-shifted emission spectrum consistent with the fluorophore identified in the retina explants. This compound was also observed to accumulate in an age-dependent manner (shown in Fig. 3, panel B). Based on the absorbance and fluorescence spectra of this species, its tissue localization, and age-dependent accumulation, it was tentatively identified as A2PE-H2, a precursor of A2E that is formed in the retina. Further analyses of this species showed that it can be sequentially converted to A2PE and A2E under acidic conditions that mimic the low pH of the phagolysosomes within RPE cells [24], thereby supporting its identification as a precursor of A2E.

The Cone-Dominant Abca4/Nrl Double Null Mutant Mouse

As described above, *Abca4*$^{-/-}$ mice share some of the disease characteristics seen in patients with STGD1, including delayed dark adaptation, enhanced retinal autofluorescence, and increased accumulation of A2E. However, because the mouse retina does not have a macula and contains only about 3%-5% cones [49], biochemical studies of *Abca4*$^{-/-}$ mice provide little information regarding the pathobiology underlying cone and macular vision loss in patients with STGD1. To address this shortcoming, a cone-dominant *Abca4*$^{-/-}$ mouse model was developed [50,51]. In this model, the neural retina leucine zipper (*Nrl*) transcription factor, which controls rod photoreceptor fate [52], was genetically deleted resulting in the conversion of rod photoreceptors to cone-like photoreceptors that express cone proteins and exhibit cone electrophysiological and structural features. The *Nrl*$^{-/-}$ retina exhibits 2 key anatomical features consistent with the human macula: (1) cones are densely packed with cone outer segments in contact with one another and without interruption of rods and (2) cone outer segments are adjacent to the RPE.

Although cone photoreceptors of the *Nrl*$^{-/-}$ mutant are not identical to wild-type murine or human cone photoreceptors, the structural and physiological features of this model provided a unique opportunity to study the effects of *ABCA*4 deficiency in the context of a cone-dominant retina. Toward this objective, investigators generated *Abca4*$^{-/-}$/*Nrl*$^{-/-}$ double knockout mice and compared structural, anatomical, physiological, and biochemical features of these mice to those observed in the single knockout strains [53]. The main structural effect observed in *Abca4*$^{-/-}$/*Nrl*$^{-/-}$ retinas was a reduction in rosette number compared with *Nrl*$^{-/-}$ retinas. Increased retinal stress, as measured by glial fibrillary acidic protein, was found in both rod- and cone-dominant retinas lacking *Abca*4. Intriguingly, the eyes of *Abca4*$^{-/-}$/*Nrl*$^{-/-}$ mice were found to generate ~6-times more A2E per mole of 11-*cis*-retinal than eyes of *Abca4*$^{-/-}$/*Nrl*$^{+/+}$ mice. Despite this, the RPE of *Abca4*$^{-/-}$/*Nrl*$^{-/-}$ eyes showed fewer lipofuscin granules (4-fold lower) compared with the RPE of *Abca4*$^{-/-}$/*Nrl*$^{+/+}$ eyes.

The higher rate of A2E biosynthesis in *Abca4*$^{-/-}$/*Nrl*$^{-/-}$ mice can be explained by the higher capacity of cones for photoisomerization prior to saturation under ambient light compared with rods (up to 1,000,000 vs. 500 photoisomerizations per second, respectively) [54,55]. Thus, cones utilize more retinoid and place a higher metabolic demand on retinoid recycling compared with rods. This effect is likely exacerbated in the macula versus peripheral retina of patients with STGD1 due to the much higher density of cone photoreceptors per RPE cell [56]. Accordingly, impairment of retinoid recycling

due to *Abca*4 deficiency in cones would be expected to generate more all-*trans* retinal and bisretinoids compared with *Abca*4 deficiency in a rod-dominant retina.
The finding of fewer lipofuscin granules in the RPE of *Abca*4$^{-/-}$/*Nrl*$^{-/-}$ eyes, despite the increased production of A2E, suggests that A2E can be generated in cones but is not taken into the RPE. Thus, A2E and/or precursor bisretinoids may abnormally remain in or be associated with the cone photoreceptor or neighboring structures where cytotoxic effects could be exerted. The ability of cone-derived bisretinoids to escape RPE phagocytosis may be attributed to the unique anatomy/structure of cone photoreceptors compared with rod photoreceptors. In rods, the outer segment discs are enclosed within a plasma membrane sheath which restricts migration of bisretinoids out of the disc, eventually to be phagocytosed by the RPE. In contrast, cone outer segment discs are contiguous with the plasma membrane, with no barrier that would restrict bisretinoid interaction with other cellular compartments. These other cellular compartments, such as the inner segment, do not turn over membrane in the same way as outer segments; therefore, A2E and related bisretinoids might be expected to accumulate in the cone cell rather than the RPE.
It is noteworthy that reduced lipofuscin accumulation observed in *Abca4*$^{-/-}$/*Nrl*$^{-/-}$ mice has also been recently reported in the cone-rich retina of zebrafish following genetic ablation of human *ABCA4* paralogues (*abca4a* and *abca4b*). In this model, absence of *abca4a* and *abca4b* results in elongation of cone outer segments (COS) and loss of a constitutively expressed and externally presented phosphatidylserine that is believed to function as an apoptotic 'eat-me' signal to trigger phagocytosis by the RPE [57]. The histological findings from this model suggest that in addition to the known transporter function of the ABCR protein, it may also play a critical structural role in COS morphology. If conserved in humans, this function of ABCR would have significant implications for our understanding of early retinal pathology and subsequent vision loss in STGD1.
Together, these data show that cones and rods possess intrinsically different responses to *ABCA4*/ACBR deficiency and suggest that macular vision loss in STGD1 may be due to both a direct toxic effect of accumulated bisretinoids on cones and, potentially, loss of COS structural integrity, rather than being entirely attributed to photoreceptor degeneration as a consequence of RPE atrophy.

Identification of Bisretinoids in Human STGD1 Retina and RPE

The early appearance of autofluorescent lesions (e.g., dots and/or flecks) is a hallmark feature of STGD1 [40,58,59]. This autofluorescence is believed to be due to an accumulation of retinoid byproducts and/or lipofuscin. Interestingly, Solberg et al. reported cases in which early appearing autofluorescent flecks which displayed short fluorescence lifetimes converted to longer fluorescence lifetime autofluorescence over time [59]. This transition indicates a change in the composition of the underlying retinoid fluorophores as the disease progresses. The longer fluorescence lifetime observed by Solberg et al. is consistent with A2E [60]; the identity of the early appearing retinoid byproduct(s) with shorter fluorescence lifetime is not entirely clear.
In an effort to identify the underlying autofluorescent compounds in STGD1, a study of retina and RPE tissue from post-mortem eyeglobes of 2 patients with STGD1 was conducted [24]. One of these patients had a diagnosis of fundus flavimaculatus (FFM), a now seldom-used term to describe late-onset STGD1. Post-mortem eyeglobes from age-matched unaffected controls were used for comparison. Retinoids were extracted from samples of retina and RPE tissue taken from the cone rich macular–perimacular region of the eyeglobes and the extracts were analyzed chromatographically and spectrally.
Chromatographic analysis of the STGD1 and FFM retina samples showed elevated levels of PE relative to the control ("normal") samples (shown in Fig. 4, panels A-C). This is consistent with ABCR as a transporter of *N*-ret-PE since impaired transport of *N*-ret-PE out of the retina would be expected to cause accumulation of PE (described in the *Introduction*). Importantly, an unusual retinoid species was identified in the STGD1 and FFM retinas that was not present in normal tissue. This compound showed a unique UV–visible absorbance spectrum with a maximum at ~500 nm (shown in Fig. 4,

panels B and C, and insets). Chemical characterization of this compound revealed that it was consistent with A2PE-H2 which had been identified in retina explants from *Abca4*$^{-/-}$ mice [27]. Analysis of the RPE samples from STGD1 and FFM tissues showed the presence of both A2PE-H2 and A2E (shown in Fig. 4, panels E and F, and panel insets); these compounds were not detected in normal age-matched RPE tissue (shown in Fig. 4, panel D). The finding that only A2PE-H2 was found in STGD1 and FFM retina samples, but not in normal retina samples, and the presence of both A2PE-H2 and A2E only in STGD1 and FFM RPE, support the hypothesis that A2PE-H2 is a precursor of A2E which is transformed following phagocytosis into the RPE. The reduced autofluorescence emission of A2PE-H2 observed in retina explants from *Abca4*$^{-/-}$ mice (shown in Fig. 2, panel A) would predict a shorter fluorescence lifetime compared with A2E, indicating that A2PE-H2 is very likely the early appearing retinoid byproduct identified by Solberg et al [59].

Relationship Between Fundus Autofluorescence and Retinal Pathology in STGD1

We turned to past clinical studies to better understand the relationship between retinal autofluorescence and photoreceptor function/integrity. Due to the lack of definitive models and methods to determine the sequence of pathophysiological changes that occur in the eyes of living patients with STGD1, studies have relied on assessing phenotypic changes, such as structural and autofluorescence changes over the course of disease development and progression to infer the order of pathological events. Various clinical studies have reported photoreceptor abnormalities and autofluorescence that precede RPE atrophy in patients with early-stage disease. These findings challenge the conventional belief that RPE atrophy precedes photoreceptor loss in STGD1.

Cellular Localization of Autofluorescence and Associated Pathology

The natural autofluorescence emission from a normal healthy fundus detected with short-wavelength autofluorescence (SW-AF, excitation 400-600 nm) is primarily due to bisretinoids within the RPE [14]. Fundus flecks observed in patients with STGD1 show a dramatically elevated SW-AF emission which implicates bisretinoid accumulation as a source [37-39]. However, it is unclear whether the SW-AF associated with flecks emanates from RPE lipofuscin or photoreceptors. A characterization of the evolution of flecks in STGD1 using multimodal imaging has been reported [48]. In this study, flecks observed in SW-AF images were seen to colocalize with foci exhibiting a reduced or absent near-infrared autofluorescence (NIR-AF). Since the NIR-AF signal is derived from melanin, with a minor contribution from choroidal melanocytes [61,62], loss of this autofluorescence is indicative of melanin loss and RPE atrophy. Flecks in SW-AF and NIR-AF images corresponded to hyperreflective lesions tracking with photoreceptor-attributable bands within the IS/OS junction (i.e, the ellipsoid zone [EZ] and external limiting membrane [ELM]) on spectral domain optical coherence tomography (SD-OCT). These hyperreflective lesions were also associated with thinning of the outer nuclear layer (ONL). On serial imaging, changes in NIR-AF preceded the onset of fleck hyperautofluorescence in SW-AF images and fleck profiles in NIR-AF images tended to be larger. Because loss of the NIR-AF signal is indicative of RPE atrophy, the SW-AF of flecks must emanate from another source. The authors noted that bisretinoids residing within photoreceptors likely serve as the source of the SW-AF signal.

The findings reported in the study described above are consistent with data from an earlier study which investigated the localization of flecks and the incongruous observation whereby flecks, presumed to originate from RPE lipofuscin, can exhibit increased SW-AF, while NIR-AF, primarily from RPE melanin, is usually reduced or absent at fleck positions [63]. The study authors suggested that the bright SW-AF emission from flecks derives from photoreceptor outer and inner segments that are degenerating secondary to RPE atrophy. Thus, the outer to inner expansion of fleck deposits in SD-OCT scans may represent progressive stages in the degeneration of photoreceptor cells within fleck areas. The observation of decreased retinal sensitivity in fleck versus non-fleck areas on microperimetric testing [64] is consistent with this theory.

The notion that SW-AF in STGD1 may emanate from inner and outer segments is further supported by histopathological findings of lipofuscin-like material in the inner segments of post-mortem STGD1

photoreceptors [44]. Additionally, evidence from the Royal College of Surgeon rat which shows abnormal accumulation of bisretinoids in photoreceptors prior to, or concurrent with, degeneration due to deficient phagocytosis [65,66] suggests that photoreceptor cells under stress may form excessive bisretinoid levels as a consequence of aberrant handling of all-*trans* retinal [14]. Finally, in mice with null mutations in both *Abca*4 and retinol dehydrogenase 8 (*Rdh8*), the inner segment/outer segment-containing core of the aberrant photoreceptor cell rosettes emit a distinct autofluorescence [67].

It is noteworthy that the localization of the SW-AF signal within photoreceptors, and the associated excitation and emission properties that have been associated with flecks, are consistent with the A2E precursors (A2PE-H2 and A2PE) which are continually produced in outer segment discs due to a dysfunctional ABCR protein. Therefore, because A2PE-H2 and A2PE would continue to be produced within photoreceptors until their demise, it seems unlikely that the corresponding SW-AF signal would appear only after loss/failure of the RPE. Rather, the observation that onset of fleck hyperautofluorescence in SW-AF images is preceded by RPE atrophy (i.e., changes in NIR-AF) suggests that melanin within functioning RPE cells or macular pigments [68,69] may interfere with visualization of the SW-AF signal within photoreceptors, perhaps due to a masking effect. Regional loss of RPE cells would presumably eliminate any masking effect revealing the SW-AF signal within photoreceptors.

Alternatively, the SW-AF signal within photoreceptors may be below the limit of detection until loss of the RPE, which would cause an increase in bisretinoid accumulation and a corresponding increase in the SW-AF signal within photoreceptors due to impaired phagocytosis by the RPE. In either case, the data show that the SW-AF signal of fundus flecks tracks with photoreceptor cell degeneration. The question that remains is whether the SW-AF signal within photoreceptors (i.e, bisretinoids) is associated with compromised photoreceptor function or integrity throughout the disease course, or if these cytotoxic effects occur only after loss of the RPE due to the increased metabolic burden placed on photoreceptors.

Photoreceptor Abnormalities Preceding RPE Loss in STGD1

In a comparison of structural changes seen on SD-OCT to those visible on FAF imaging in 22 eyes of 11 patients with STGD1, diameter measurements of foveal inner and outer segment (IS/OS) junction and RPE atrophy on transverse OCT b-scans were examined [38]. This analysis showed that the diameter of absent FAF was smaller than the extent of EZ loss in all but 3 eyes. However, when the transition zone between the region of absent FAF (indicating RPE atrophy) and normal FAF was considered, the area closely approximated the IS/OS junction loss measurement. Since IS/OS junction loss implies loss of photoreceptor functioning, the finding that the region of IS/OS loss was larger than the region of absent FAF suggests that photoreceptor loss is occurring in the absence of RPE atrophy. The study authors also noted that for 3 patients, photoreceptor abnormalities were observed within the fovea on SD-OCT without an equivalent abnormality on FAF at the level of the RPE. The investigators also identified 1 eye of a patient, presumably at the initial stage of the disease, which had normal FAF, but showed disorganization of the photoreceptor layer and outer retinal layers on SD-OCT.

The findings described above have been corroborated by other investigators [70-72]. In these studies, OCT imaging and sub-RPE slab projection methods were utilized to create *en face* images of RPE atrophy by visualizing light penetration into the choroid. The extent of RPE atrophy and IS/OS attenuation and their relationship was examined. Whereas Melillo, et al. [70] measured the transverse extents of IS/OS loss on OCT b-scans, as in the earlier study by Gomes et al. [38] described above, both Sodi, et al. [71] and Greenstein, et al. [72] utilized slab methods to produce *en face* projections of the IS/OS layer. Despite the differing methods and different cohort sizes (Melillo et al., n=98; Gomes et al., n=11; Sodi et al., n=32; Greenstein et al., n=16), all 4 groups found that the extent of IS/OS junction loss was greater than the extent of RPE atrophy.

In a more recent study conducted by Alabduljalil et al. [73], *en face* OCT and OCT angiography imaging, which incorporated an *en face* slab projection method with boundary maps, was used to visualize IS/OS loss and RPE atrophy masks that delineated areas of loss. This method, which measures an apical RPE signal that may be more sensitive to a wider spectrum of RPE thinning compared with sub-RPE methods, permits an analysis of total IS/OS junction loss or RPE atrophy, regions with isolated IS/OS junction loss, isolated RPE atrophy, matched IS/OS junction and RPE degeneration, or intact IS/OS junction and RPE. The imaging data from this analysis showed a strong correlation between photoreceptor and RPE degeneration wherein IS/OS junction loss was 1.6-fold greater than the area of RPE atrophy, supporting the theory that photoreceptor degeneration precedes RPE atrophy in STGD1. Similar findings have been reported in patients with childhood-onset STGD1 in which the rate of IS/OS junction loss was found to be 1.7-times higher than the rate of change in the total FAF area (i.e., decreased autofluorescence) [74,75].

It is important to note that studies which implicate lipofuscin accumulation in the RPE as the primary pathological event leading to progressive photoreceptor cell death have been reported. There are 2 notable studies. In the first study by Cideciyan et al. [76], surrogate measures of lipofuscin accumulation, photoreceptor and RPE loss, and retinoid cycle kinetics were evaluated in order to determine the relationship between these phenotypic features. The study included 47 patients (mean age ± SD of 39 ± 16 years) representing a wide spectrum of *ABCA*4-related autosomal recessive forms of human blindness due to retinal degeneration (RD) including STGD1. The extent of lipofuscin accumulation was measured using quantitative autofluorescence (qAF) with excitation at 488 nm and fluorescence detection above 500 nm. Measures of rod and cone cell death were made using visual field data from a modified automated perimeter, and measures of rod adaptation delay were used to assess retinoid cycle slowing. The study authors noted that increased qAF intensity was the only abnormality that occurred in early-stage disease (Stages I-II). Further increase of qAF in Stage III was associated with increased autofluorescence texture, which was taken as a measure of RPE cell death, and decline of qAF in Stages IV-V coincided with death of rod and cone photoreceptors and delayed rod dark adaptation. These data suggest that elevated RPE lipofuscin may be the first pathophysiological process detectable in human ABCA4-RD and that loss of the RPE precedes photoreceptor cell loss.

In a similar study by Muller et al. [12], qAF measures were correlated with demographic characteristics, structural alterations observed on OCT and FAF, retinal function measured using best corrected visual acuity (BCVA), ERG and perimetry, and genotype in 77 patients with *ABCA*4-related retinopathy (mean age ± SD of 34 ± 15 years) and 110 control subjects. The study authors noted that qAF scores were particularly high in younger patients with *ABCA*4-related retinopathy, and only slightly elevated in older patients. Importantly, there was no consistent correlation between BCVA and qAF score in patients with *ACBA*4-related retinopathy because most patients had already lost central vision early in disease progression, regardless of qAF value. In some patients, qAF was observed to be in the range of ceiling levels; however, full-field ERG responses and fundus-controlled perimetry measures were still in the normal range. This observation corroborates the conclusion by Cideciyan et al. [76] that increased AF intensity is the only abnormality that occurs while assessments for all other parameters were within normal values.

In both studies described above, the investigators used autofluorescence intensity on qAF imaging with 488 nm excitation as a surrogate measure of lipofuscin. It is important to note that oxidized melanin possesses an intrinsic fluorescence emission (above 500 nm) that is maximally excited at approximately 470 nm [77]. Thus, the 488 nm excitation light used for qAF imaging would also produce fluorescence from oxidized melanin in the RPE. Given the mean age of the patients from the aforementioned studies (34-39 years), and the described disease severity, the presence of oxidized melanin is likely and could be a confounding variable of this approach. Additionally, since high-resolution, cross-sectional images of the retina were not collected in either study, the exact source of the observed qAF signal cannot be confirmed (i.e., there could be contributions from retinal cell

layers other than the RPE). Finally, because the described studies were cross-sectional, rather than longitudinal, it is difficult to relate disease severity among patients to the observed phenotypes. In fact, Cideciyan et al. [76] noted that the retina-wide index of disease severity did not correlate with the proposed disease stage, except for the final stage. Thus, given the wide spectrum of disease phenotypes that are associated with *ABCA*4 variants, the reported findings may not be applicable to all patients. The comment by Muller et al. [12] that the accumulation of lipofuscin precedes other structural changes in some, but not all, patients, suggests that this chronology of pathology may be manifest only in a subgroup of patients harboring specific *ABCA*4 variants.

Collectively, these data support a potential sequence wherein dysfunction of the ABCR protein leads to the accumulation of cytotoxic bisretinoids which may directly or indirectly affect photoreceptor function and integrity. While damage and atrophy to the RPE certainly contribute to the degenerative process in STGD1, the anatomical data suggest that it is clearly not the only causative factor in underlying photoreceptor degeneration in STGD1.

Peripapillary Sparing in STGD1

An interesting feature of retinal pathology in STGD1 is peripapillary sparing, characterized by the absence of flecks and RPE atrophy in the peripapillary region of the retina, even at advanced disease stages [78-80]. This region between the fovea and optic nerve head has been shown to be commonly used as the preferred fixation locus in patients with STGD1 when central vision is lost [78] providing an impetus for structural and functional characterization of this region. In one such study, investigators used FAF and SD-OCT imaging to evaluate the integrity of the outer retinal layers and RPE and microperimetry to assess visual function in the peripapillary region and across the macula in 27 patients with STGD1 and 12 age-similar controls [80]. Patients were categorized into groups based on ERG profiles (ERG group I, normal scotopic and photopic ERGs; ERG group II, decreased photopic ERGs; ERG group III, decreased scotopic and photopic ERGs). Due to eccentricity and instability of fixation in patients with ERG group III disease, these data were excluded. The thicknesses of the outer nuclear layer plus outer plexiform layer (ONL+), outer segment (OS), and RPE were measured through the fovea, and peripapillary areas in patients with ERG group I and II disease.

Among the 27 patients with STGD1, 14 had disease confined to the central macula. In these patients, there was significant thinning of the ONL+ and OS layers in regions where RPE layer thickness and FAF were normal, although the RPE layer thicknesses were at the lower end of normal. This finding provides additional evidence that changes in the photoreceptor layer may precede the development of abnormalities in the RPE. Only 2 patients showed significant thinning of the ONL+ and OS layers across the entire peripapillary region. These 2 patients demonstrated abnormalities on FAF surrounding the optic disc, as well as having ERG group II disease, indicating that lipofuscin accumulation likely preceded photoreceptor abnormalities in these patients.

The reason for peripapillary sparing remains unclear. This area may be more resilient to the deleterious effects of *ABCA*4 variants due to a more favorable RPE to photoreceptor ratio which would be expected to result in reduced bisretinoid/lipofuscin accumulation. The dramatic decrease in photoreceptor density from the periphery to the normal peripapillary zone (from ~140,000 to ~65,000 cells/mm^2) that has been observed in human eyes [81] could produce a constitutively lower rate of bisretinoid accumulation. This would relieve the disc membrane load placed upon peripapillary RPE cells making them less vulnerable to the effects of excessive accumulation of both bisretinoids and lipofuscin.

Retinal Pathology in Early-Stage STGD1

Longitudinal assessment of patients with early-stage disease has also helped shed light on the sequence of pathophysiological events in STGD1. In a 27-month study of disease progression in STGD1, high-resolution adaptive optics scanning laser ophthalmoscopy (AOSLO) was used to correlate cone photoreceptor structure with FAF images (excitation = 488 nm) and visual function [47]. Among the 12 patients enrolled in the study, 3 presented with early-stage disease. Two of these 3 patients exhibited minimal or no RPE abnormalities but displayed abnormal cone

morphology/packing structure and photoreceptor layer morphology which coincided with increased FAF. In 1 patient with early-stage disease, RPE cells were determined to be present; however, a loss of foveal cones and a concurrent reduction in VA was observed. Longitudinal assessment of a second early-stage patient revealed reduced retinal sensitivity by microperimetry which was accompanied by an increase in hyperautofluorescent spots and cone spacing abnormalities at the fovea. The authors noted that among the 12 patients in the study, all instances of RPE atrophy were accompanied by cone spacing abnormalities. However, there were several instances of cone spacing abnormalities and photoreceptor cell autofluorescence in the presence of intact RPE. The authors concluded that the observed correlation between abnormal FAF and abnormalities in cone morphology and packing structure, in the absence of RPE atrophy, indicates a direct correlation between increased FAF and loss of cone photoreceptors.

The findings described above are consistent with data from another study that was conducted to characterize the sequence of events that ultimately result in RPE and photoreceptor cell death in STGD1. In this study, investigators chose to study the earliest stages of the disease by examining a cohort of children with STGD1 before the development of macular atrophy [82]. Eight children (median age, 8.5 years) without macular atrophy were identified. All children harbored biallelic *ABCA4* variants: 4 were asymptomatic and 4 reported loss of VA. At presentation, the macula appeared normal in 3 children, 4 children had a subtly altered foveal reflex, and 1 child demonstrated manifest fine yellow dots. Complimentary structural and functional tests (OCT, FAF, AOSLO, ERG) were used to identify a number of novel characteristics. One of the earliest structural changes that was evident on the OCT images of all patients was in the ONL. The OCT images revealed an increase in reflectivity extending internally from the line thought to correspond to the ELM which separates the inner segments of the photoreceptors from the ONL. The thickness of this change was at a maximum at the foveola and appeared to decline steadily toward the foveal avascular zone where it became invisible. This OCT abnormality, termed ELM thickening, was also associated with a buildup of hyperreflective deposits in the ONL, presumably from degenerating photoreceptor cells [83]. The study investigators noted that the identified changes are transient and likely the result of pathologic disruption of cones within the outer lamella of the ONL. This conclusion was based on the correspondence between the patten of ELM thickening to the spatial distribution of cone photoreceptors. Unlike rod nuclei which are thought to be distributed throughout the entire thickness of the ONL, cone photoreceptor nuclei have defined spatial distribution, being most numerous and tightly packed at the fovea and less densely packed in the perifoveal retina [84]. Sequential imaging showed that where significant numbers of photoreceptor nuclei were lost, collapse of the inner retinal layers into the ONL seemed to occur preferentially at perifoveal loci, sparing the foveola. This pattern of degeneration was also evident on AOSLO where the greatest increase in cone spacing occurred in the parafoveal region, with relative sparing of the foveolar cones. Notably, all patients retained a degree of physiological hypoautofluorescence, and foveolar autofluorescence was relatively well-preserved, indicating that structures important for imparting these characteristics, the RPE and macular pigments, remain relatively intact. This is also consistent with the hypothesis that perifoveal disease occurs first in STGD1.

It is tempting to speculate that the foveal sparing phenotype may be due to the high density of cones in this region [56], and the greater capacity of cones for visual pigment regeneration, compared with rods [54,55]. The finding that the rate of visual chromophore regeneration within the RPE is insufficient to support the rapid dark-adaption of cones has led to the identification and characterization of an alternate, RPE-independent, source of cone-specific chromophore (11-*cis* retinol) which can be utilized by Müller cells to regenerate visual pigment [85]. It is also significant that the ratio of Müller cells to cones in the primate fovea has been found to be 1:1, indicating a more functionally intimate relationship between the two cell types [86]. Thus, ELM thickening could be a compensatory cellular response to the presence of bisretinoid-laden photoreceptor and/or RPE cells in an effort to maintain interaction between Müller cells and cone photoreceptors.

Interestingly, FAF imaging in the cohort of STGD1 children without macular atrophy revealed 2 discrete patterns of hyperautofluorescence: classical pisciform flecks that do not encroach on the foveola, and tiny discrete dots that never extend outside the foveola. Although both lesions eventually evolve to outer retinal atrophy, they may do so at different rates. This observation could be readily explained by the presence of 2 distinct pathways for visual chromophore regeneration: (1) an intraretinal pathway involving Müller and cone cells, and (2) an intra-RPE pathway which supports rods. Thus, the tiny hyperautofluorescent dots may be wholly intraretinal, whereas the larger flecks are present in the RPE and photoreceptor outer segments. This hypothesis would be consistent with prior studies that have identified autofluorescent deposits in cone inner segments and in Müller cell processes, as well as within the RPE [44,87]. The OCT and FAF data provided by this study support the hypothesis that cone photoreceptor dysfunction is intrinsic to the disease process and not secondary to RPE failure.

Lastly, a cross-sectional study was conducted to identify the sources of autofluorescence signals in STGD1 using high-resolution *in vivo* images of cones, rods, and RPE cells [39]. This study, which included 3 patients with STGD1 showing central VA loss, combined single-cell resolution confocal reflectance AOSLO images with fluorescence AOSLO (FAOSLO) images. Of note, this study utilized short wavelength FAOSLO (excitation = 532 nm; emission = 575 to 725 nm), which would elicit autofluorescence from the A2E precursor, A2PE-H2. Imaging of the transition zone (i.e., the area outside the clinically apparent macular atrophic lesion) in these subjects revealed abnormally enlarged rods and cones and abnormal autofluorescence. The authors commented that the autofluorescence signal was atypical of RPE cell mosaics and suggested that hyperautofluorescence at the leading disease front in STGD1 may be due to the accumulation of bisretinoid precursors within photoreceptors, or a combination of photoreceptor and RPE cells, and may represent an early disease stage in STGD1.

Altogether, the reviewed clinical studies offer evidence that photoreceptor abnormalities and associated autofluorescence can precede RPE atrophy and may result in loss of VA in the absence of RPE atrophy. Findings from AOSLO and FAOSLO imaging further support findings from studies of *Abca4*$^{-/-}$ mice and post-mortem eyeglobes, which show that autofluorescence emanating from the retina and RPE are distinct due to the different bisretinoid species in these compartments.

Visual Function Loss Preceding RPE Atrophy in Early-Stage STGD1

The clinical studies described above support the theory that bisretinoid species within photoreceptors may be responsible for early anatomical and structural changes which precede atrophy of the RPE. Bisretinoids accumulate early in the disease process and produce a distinct hyperautofluorescence emission which can be detected by FAF imaging. The international multicenter Progression of Atrophy Secondary to Stargardt Disease (ProgStar) study aimed to understand the natural history of disease progression in STGD1. The primary objective was to assess the yearly rate of progression of STGD1 using the growth or the development of atrophic lesions as measured by FAF imaging [88]. The ProgStar Study Group defined lesions of abnormally reduced autofluorescence as definitely decreased autofluorescence (DDAF; >90% darkness relative to the optic nerve head), questionably decreased autofluorescence (QDAF; between 50-90% darkness) and decreased autofluorescence (DAF; the sum of DDAF and QDAF). DDAF lesions are considered atrophic, representing RPE and/or photoreceptor cell death which is likely to lead to progressive loss of visual function, while QDAF lesions may or may not be associated with RPE atrophy [89].

While the impact of QDAF lesions on visual function has not been systematically studied, it is widely accepted that QDAF lesions are due to bisretinoid species within the retina and RPE, and they precede the appearance of DDAF lesions. In fact, lesion growth data from the prospective ProgStar natural history study of STGD1, which focused on recent-onset STGD1 (i.e., onset of symptoms ≤2 years before the first visit), confirmed that early-appearing QDAF lesions transition over time to atrophic DDAF lesions [88]. Data from that study showed a statistically significant association (P<0.001) between the regression (decrease) in QDAF area over time and increased growth in DDAF

area. This inverse relationship strongly suggests that as hyperautofluorescent QDAF areas diminish, they are effectively converting into DDAF lesions with reduced autofluorescence. A key point of interest is whether QDAF lesions are associated with visual function deficits. To address this, an analysis of visual function in early-stage STGD1 patients who show only QDAF lesions at baseline is required.

A survey of recent STGD1 clinical studies posted on ClinicalTrials.gov reveals that a study in adolescent STGD1 patients showing QDAF lesions at baseline has been conducted. This trial was a 2-year, open-label, Phase 2 study which was conducted to evaluate safety and tolerability of an orally administered small molecule drug (Tinlarebant) that is intended to slow bisretinoid biosynthesis in the retina by reducing retinol delivery to the eye (NCT05266014). The trial enrolled 13 adolescent subjects aged 12-18 years. Although the final 2-year data from this study have not yet been published, details of the study design and patient characteristics have been presented at key ophthalmology conferences. Genetic analyses revealed biallelic pathogenic or likely pathogenic *ABCA*4 mutations in all study subjects and baseline FAF assessments showed only QDAF lesions which were either in, or adjacent to, the fovea in all subjects. Analysis of the 2-year BCVA data from this study may be very useful to determine whether QDAF lesions alone (i.e., bisretinoids) are associated with compromised visual function.

Conclusion

The clinical findings described in this review are consistent with preclinical data from STGD1 mouse models which suggest that A2PE-H2 may be the primary source of autofluorescence and potential cytotoxicity in photoreceptor cells of patients with STGD1. The *in vitro* conversion of A2PE-H2 to A2E under low pH conditions mimicking that of the phagolysosomes within RPE cells, and the findings of A2PE-H2 in post-mortem STGD1 retinas, and both A2PE-H2 and A2E in post-mortem STGD1 RPE tissue, further implicate A2PE-H2 as the precursor of A2E. While the cytotoxicity of A2E in the RPE has been well documented, nothing is known regarding the potential cytotoxicity of A2PE-H2 and related bisretinoids in photoreceptors.

Characterizations of the evolution of flecks in STGD1 have shown that the SW-AF emanating from flecks, in the absence of RPE atrophy, could be due to bisretinoids residing within photoreceptors. Notably, the change in fluorescence lifetime of flecks during the outer to inner expansion through retinal tissue is consistent with the formation of highly fluorescent A2E in the RPE from a weakly fluorescent A2PE-H2 precursor in photoreceptors. Importantly, reduction in retinal sensitivity in fleck versus non-fleck areas on microperimetric testing could be explained by an intrinsic cytotoxicity of flecks. This finding could also be due to degenerating RPE (as evidenced by the dark flecks on NIR-AF) with limited phagocytotic ability and accompanying photoreceptor degeneration, leading to secondary accumulation of autofluorescent subretinal debris. In either case, it is notable that numerous studies have documented specific anatomical and structural changes in the retina that occur in the context of increased FAF and photoreceptor abnormalities on OCT, but in the absence of RPE atrophy. These alterations involve the ONL and include IS/OS junction loss and ELM thickening. Thus, the anatomical data suggests that degeneration or loss of the RPE is not the only causative factor underlying photoreceptor degeneration in STGD1.

The formation and accumulation of A2PE-H2 occurs early in the disease course and leads to RPE atrophy over time. However, since the majority of reported STGD1 cases manifest macular atrophy at time of diagnosis, there is little information about earlier stages of disease. Similarly, nearly all past and current interventional clinical trials in STGD1 have enrolled adult subjects with advanced disease. Primary efficacy endpoints in these clinical trials have focused on slowing RPE atrophy or ameliorating pathology which occurs secondary to RPE atrophy (e.g., changes in EZ defect area). Based on the biology of disease in STGD1 and the accompanying evolution of various bisretinoid species, clinical investigation of pathogenesis in early-onset STGD1 could be very informative. For example, longitudinal assessment of patients with early-stage STGD1 has revealed a correlation between abnormal FAF and abnormalities in cone morphology and packing structure, in the absence

of RPE atrophy, indicating a direct correlation between increased FAF and loss of cone photoreceptors. Similar findings were reported in a study of childhood-onset STGD1 in which alterations in the ONL and ELM were observed prior to the development of macular atrophy. These clinical findings provide an impetus to determine whether loss of visual function in childhood-onset STGD1 subjects who show only QDAF lesions and no RPE atrophy is due to the gradual accumulation of bisretinoids within photoreceptors. An analysis of the relationship between changes in QDAF and DDAF area versus BCVA loss in early-stage disease would be very informative.

The autofluorescence of QDAF lesions represents one of the earliest signs of impending retinal atrophy in STGD1. Therefore, a therapeutic intervention which is directed at slowing the expansion of QDAF lesions may have a greater long-term benefit for patients since it could potentially slow the onset/growth of atrophic retinal lesions and preserve visual function at an earlier stage of disease. In this respect, slowing the growth of QDAF lesions, or slowing the transition from QDAF to DDAF lesions, may represent surrogate endpoints for eventual vision loss, similar to slowing RPE and photoreceptor atrophy which are currently accepted as primary efficacy endpoints. As noted, other early indicators of worsening retinal disease in STGD1 include thickening of the outer retina and formation/migration of flecks. Findings of increased FAF in these affected areas also implicates excess bisretinoid accumulation, further supporting use as biomarkers or potential surrogate endpoints for disease progression.

The disease biology and sequence of pathogenesis in STGD1 suggests that a therapy which is effective to reduce bisretinoid formation/accumulation would be expected to slow the formation of retinal lesions, preserving visual function, and improving the quality of life for affected patients. Until an approved therapy is available, the avoidance of risk factors which exacerbate bisretinoid toxicity (e.g., excessive vitamin A intake, exposure to UV light and oxidative stressors, such as smoking) may be effective in slowing disease progression.

Acknowledgements

The authors would like to acknowledge Belite Bio, Inc. for support in the preparation of this manuscript

Conflict of Interest Statement

NL Mata and HPN Scholl are employees of Belite Bio, Inc. C Rivolta and HPN Scholl were members of the journal's Editorial Board at the time of submission. No other conflicting relationship exists for any author.

Funding Sources

Belite Bio, Inc. provided support for preparation of the manuscript.

Author Contributions

NL Mata led the development of the manuscript with authorship and literature review support from S Weng. M Quinodoz and C Rivolta contributed STGD1 prevalence data and text. M Michaelides, PC Issa, M Quinodoz, C Rivolta, and HPN Scholl provided expert review of the manuscript. All authors approved the final version of the manuscript.

References

1. Blacharski PA. Fundus flavimaculatus. In: Newsome DA. Retinal Dystrophies and Degenerations. New York: Raven Press; 1988. p. 135-159.
2. Lambertus S, Lindner M, Bax NM, et al. Progression of Late-Onset Stargardt Disease. Invest Ophthalmol Vis Sci. 2016;57(13):5186-5191.
3. Rotenstreich Y, Fishman GA, Anderson RJ. Visual acuity loss and clinical observations in a large series of patients with Stargardt disease. Ophthalmology. 2003;110(6):1151-8.
4. McBain VA, Townend J, Lois N. Progression of retinal pigment epithelial atrophy in stargardt disease. Am J Ophthalmol. 2012;154(1):146-54.
5. Fujinami K, Zernant J, Chana RK, et al. Clinical and molecular characteristics of childhood-onset Stargardt disease. Ophthalmology. 2015;122(2):326-34.
6. Westeneng-van Haaften SC, Boon CJ, Cremers FP, et al. Clinical and genetic characteristics of late-onset Stargardt's disease. Ophthalmology. 2012;119(6):1199-210.
7. Fujinami K, Sergouniotis PI, Davidson AE, et al. Clinical and molecular analysis of Stargardt disease with preserved foveal structure and function. Am J Ophthalmol. 2013;156(3):487-501.e1.
8. Cremers FPM, Lee W, Collin RWJ, et al. Clinical spectrum, genetic complexity and therapeutic approaches for retinal disease caused by ABCA4 mutations. Prog Retin Eye Res. 2020;79:100861.
9. Allikmets R, Singh N, Sun H, et al. A photoreceptor cell-specific ATP-binding transporter gene (ABCR) is mutated in recessive Stargardt macular dystrophy. Nat Genet. 1997;15(3):236-46.
10. Molday RS, Zhong M, Quazi F. The role of the photoreceptor ABC transporter ABCA4 in lipid transport and Stargardt macular degeneration. Biochim Biophys Acta. 2009;1791(7):573-83.
11. Wielgus AR, Chignell CF, Ceger P, et al. Comparison of A2E cytotoxicity and phototoxicity with all-trans-retinal in human retinal pigment epithelial cells. Photochem Photobiol. 2010;86(4):781-91.
12. Müller PL, Gliem M, McGuinnes M, et al. Quantitative Fundus Autofluorescence in ABCA4-Related Retinopathy -Functional Relevance and Genotype-Phenotype Correlation. Am J Ophthalmol. 2021;222:340-350.
13. Cideciyan AV, Aleman TS, Swider M, et al. Mutations in ABCA4 result in accumulation of lipofuscin before slowing of the retinoid cycle: a reappraisal of the human disease sequence. Hum Mol Genet. 2004;13(5):525-34.
14. Sparrow JR, Yoon KD, Wu Y, et al. Interpretations of fundus autofluorescence from studies of the bisretinoids of the retina. Invest Ophthalmol Vis Sci. 2010;51(9):4351-7.
15. Quazi F, Molday RS. ATP-binding cassette transporter ABCA4 and chemical isomerization protect photoreceptor cells from the toxic accumulation of excess 11-cis-retinal. Proc Natl Acad Sci U S A. 2014;111(13):5024-9.
16. Hanany M, Rivolta C, Sharon D. Worldwide carrier frequency and genetic prevalence of autosomal recessive inherited retinal diseases. Proc Natl Acad Sci U S A. 2020;117(5):2710-2716.
17. Xiao Q, Lauschke VM. The prevalence, genetic complexity and population-specific founder effects of human autosomal recessive disorders. NPJ Genom Med. 2021;6(1):41.
18. Kim SR, Fishkin N, Kong J, et al. Rpe65 Leu450Met variant is associated with reduced levels of the retinal pigment epithelium lipofuscin fluorophores A2E and iso-A2E. Proc Natl Acad Sci U S A. 2004;101(32):11668-11672.
19. Issa PC, Barnard AR, Singh MS, et al. Fundus autofluorescence in the Abca4(-/-) mouse model of Stargardt disease--correlation with accumulation of A2E, retinal function, and histology. Invest Ophthalmol Vis Sci. 2013;54(8):5602-5612.
20. Runhart EH, Sangermano R, Cornelis SS, et al. The Common ABCA4 Variant p.Asn1868Ile Shows Nonpenetrance and Variable Expression of Stargardt Disease When Present in trans With Severe Variants. Invest Ophthalmol Vis Sci. 2018;59(8):3220-3231.
21. Radu RA, Yuan Q, Hu J, et al. Accelerated accumulation of lipofuscin pigments in the RPE of a mouse model for ABCA4-mediated retinal dystrophies following Vitamin A supplementation. Invest Ophthalmol Vis Sci. 2008;49(9):3821-3829.

22. Cornelis SS, Runhart EH, Bauwens M, et al. Personalized genetic counseling for Stargardt disease: Offspring risk estimates based on variant severity. Am J Hum Genet. 2022;109(3):498-507.
23. Weng J, Mata NL, Azarian SM, et al. Insights into the function of Rim protein in photoreceptors and etiology of Stargardt's disease from the phenotype in abcr knockout mice. Cell. 1999;98(1):13-23.
24. Mata NL, Weng J, Travis GH. Biosynthesis of a major lipofuscin fluorophore in mice and humans with ABCR-mediated retinal and macular degeneration. Proc Natl Acad Sci U S A. 2000;97(13):7154-9.
25. Sparrow JR, Gregory-Roberts E, Yamamoto K, et al. The bisretinoids of retinal pigment epithelium. Prog Retin Eye Res. 2012;31(2):121-35.
26. Kwon W, Freeman SA. Phagocytosis by the Retinal Pigment Epithelium: Recognition, Resolution, Recycling. Front Immunol. 2020;11:604205.
27. Bui TV, Han Y, Radu RA, et al. Characterization of native retinal fluorophores involved in biosynthesis of A2E and lipofuscin-associated retinopathies. J Biol Chem. 2006;281(26):18112-9.
28. Finnemann SC, Leung LW, Rodriguez-Boulan E. The lipofuscin component A2E selectively inhibits phagolysosomal degradation of photoreceptor phospholipid by the retinal pigment epithelium. Proc Natl Acad Sci U S A. 2002;99(6):3842-7.
29. Parmar VM, Parmar T, Arai E, et al. A2E-associated cell death and inflammation in retinal pigmented epithelial cells from human induced pluripotent stem cells. Stem Cell Res. 2018;27:95-104.
30. Zhou J, Jang Y, Kim SR, Sparrow JR. Complement activation by photooxidation products of A2E, a lipofuscin constituent of the retinal pigment epithelium. Proc Natl Acad Sci U S A. 2006;103(44):16182-7.
31. Iriyama A, Inoue Y, Takahashi H, et al. A2E, a component of lipofuscin, is pro-angiogenic in vivo. J Cell Physiol. 2009;220(2):469-75.
32. Sparrow JR, Nakanishi K, Parish CA. The lipofuscin fluorophore A2E mediates blue light-induced damage to retinal pigmented epithelial cells. Invest Ophthalmol Vis Sci. 2000;41(7):1981-9.
33. Mihai DM, Washington I. Vitamin A dimers trigger the protracted death of retinal pigment epithelium cells. Cell Death Dis. 2014;5(7):e1348.
34. Haralampus-Grynaviski NM, Lamb LE, Clancy CM et al. Spectroscopic and morphological studies of human retinal lipofuscin granules. Proc Natl Acad Sci U S A. 2003;100(6):3179-84.
35. Stargardt K. Über familiäre, progressive Degeneration in der Maculagegend des Auges. Graefes Arhiv für Ophthalmologie. 1909;71:534-550.
36. Armstrong JD, Meyer D, Xu S, et al. Long-term follow up of Stargardt's disease and fundus flavimaculatus. Ophthalmology. 1998;105(3):448-457.
37. Lois N, Halfyard AS, Bird AC, et al. FW. Fundus autofluorescence in Stargardt macular dystrophy-fundus flavimaculatus. Am J Ophthalmol. 2004;138(1):55-63.
38. Gomes NL, Greenstein VC, Carlson JN, et al. A comparison of fundus autofluorescence and retinal structure in patients with Stargardt disease. Invest Ophthalmol Vis Sci. 2009;50(8):3953-9.
39. Song H, Rossi EA, Yang Q, et al. High-Resolution Adaptive Optics in Vivo Autofluorescence Imaging in Stargardt Disease. JAMA Ophthalmol. 2019;137(6):603-609.
40. Cukras CA, Wong WT, Caruso R, et al. Centrifugal expansion of fundus autofluorescence patterns in Stargardt disease over time. Arch Ophthalmol. 2012;130(2):171-9.
41. Fujinami K, Waheed N, Laich Y, et al. Stargardt macular dystrophy and therapeutic approaches. Br J Ophthalmol. 2024;108(4):495-505.
42. Sisk RA, Leng T. Multimodal imaging and multifocal electroretinography demonstrate autosomal recessive Stargardt disease may present like occult macular dystrophy. Retina. 2014;34(8):1567-75.
43. Ritter M, Zotter S, Schmidt WM, et al. Characterization of stargardt disease using polarization-sensitive optical coherence tomography and fundus autofluorescence imaging. Invest Ophthalmol Vis Sci. 2013;54(9):6416-25.
44. Birnbach CD, Järveläinen M, Possin DE, et al. Histopathology and immunocytochemistry of the neurosensory retina in fundus flavimaculatus. Ophthalmology. 1994;101(7):1211-9.
45. Cicinelli MV, Rabiolo A, Brambati M, et al. Factors Influencing Retinal Pigment Epithelium-Atrophy Progression Rate in Stargardt Disease. Transl Vis Sci Technol. 2020;9(7):33.

46. Boulton M, Dayhaw-Barker P. The role of the retinal pigment epithelium: topographical variation and ageing changes. Eye (Lond). 2001;15(Pt 3):384-9.
47. Chen Y, Ratnam K, Sundquist SM, et al. Cone photoreceptor abnormalities correlate with vision loss in patients with Stargardt disease. Invest Ophthalmol Vis Sci. 2011;52(6):3281-92.
48. Paavo M, Lee W, Allikmets R, et al. Photoreceptor cells as a source of fundus autofluorescence in recessive Stargardt disease. J Neurosci Res. 2019;97(1):98-106.
49. Haverkamp S, Wässle H, Duebel J, et al. The primordial, blue-cone color system of the mouse retina. J Neurosci. 2005;25(22):5438-45.
50. Mears AJ, Kondo M, Swain PK, et al. Nrl is required for rod photoreceptor development. Nat Genet. 2001;29:447-452.
51. Daniele LL, Lillo C, Lyubarsky AL, et al. Cone-like morphological, molecular, and electrophysiological features of the photoreceptors of the Nrl knockout mouse. Invest Ophthalmol Vis Sci. 2005;46:2156-67.
52. Hao H, Tummala P, Guzman E, et al. The transcription factor neural retina leucine zipper (NRL) controls photoreceptor-specific expression of myocyte enhancer factor Mef2c from an alternative promoter. J Biol Chem. 2011;286(40):34893-902.
53. Conley SM, Cai X, Makkia R, et al. Increased cone sensitivity to ABCA4 deficiency provides insight into macular vision loss in Stargardt's dystrophy. Biochim Biophys Acta. 2012;1822(7):1169-79.
54. Baylor DA, Nunn BJ, Schnapf JL. The photocurrent, noise and spectral sensitivity of rods of the monkey Macaca fascicularis. J Physiol. 1984;357:575-607.
55. Perry RJ, McNaughton PA. Response properties of cones from the retina of the tiger salamander. J Physiol. 1991;433:561-587.
56. Curcio CA, Sloan KR, Kalina RE, Hendrickson AE. Human photoreceptor topography. J Comp Neurol. 1990;292(4):497-523.
57. Willoughby JJ, Jensen AM. Abca4, mutated in Stargardt disease, is required for structural integrity of cone outer segments. Dis Model Mech. 2025;18(1):DMM052052.
58. Burke TR, Duncker T, Woods, RL, et al. Quantitative fundus autofluorescence in recessive Stargardt disease. Invest Ophthalmol Vis Sci. 2014;55(5):2841-52.
59. Solberg Y, Dysli C, Escher P, et al. RETINAL FLECKS IN STARGARDT DISEASE REVEAL CHARACTERISTIC FLUORESCENCE LIFETIME TRANSITION OVER TIME. Retina. 2019;39(5):879-888.
60. Palczewska G, Boguslawski J, Stremplewski P, et al. Noninvasive two-photon optical biopsy of retinal fluorophores. Proc Natl Acad Sci U S A. 2020;117(36):22532-22543.
61. Keilhauer CN, Delori FC. Near-infrared autofluorescence imaging of the fundus: visualization of ocular melanin. Invest Ophthalmol Vis Sci. 2006;47(8):3556-64.
62. Schmitz-Valckenberg S, Lara D, Nizari S, et al. Localisation and significance of in vivo near-infrared autofluorescent signal in retinal imaging. Br J Ophthalmol. 2011;95(8):1134-9.
63. Sparrow JR, Marsiglia M, Allikmets R, et al. Flecks in Recessive Stargardt Disease: Short-Wavelength Autofluorescence, Near-Infrared Autofluorescence, and Optical Coherence Tomography. Invest Ophthalmol Vis Sci. 2015;56(8):5029-39.
64. Verdina T, Tsang SH, Greenstein VC, et al. Functional analysis of retinal flecks in Stargardt disease. J Clin Exp Ophthalmol. 2012;3:10.4172/2155-9570.1000233.
65. Matthes MT, La Vail MM. Inherited retinal dystrophy in the RCS rat: composition of the outer segment debris zone. Prog Clin Biol Res. 1989;314:315-30.
66. D'Cruz PM, Yasumura D, Weir J, et al. Mutation of the receptor tyrosine kinase gene Mertk in the retinal dystrophic RCS rat. Hum Mol Genet. 2000;9:645-51.
67. Flynn E, Ueda K, Auran E, Sullivan JM, Sparrow JR. Fundus autofluorescence and photoreceptor cell rosettes in mouse models. Invest Ophthalmol Vis Sci. 2014;55(9):5643-52.
68. Istrate M, Vlaicu B, Poenaru M, et al. Photoprotection role of melanin in the human retinal pigment epithelium. Imaging techniques for retinal melanin. Rom J Ophthalmol. 2020;64(2):100-104.
69. Lima VC, Rosen RB, Farah M. Macular pigment in retinal health and disease. Int J Retina Vitreous. 2016;2:19.

70. Melillo P, Testa F, Rossi S, et al. En Face Spectral-Domain Optical Coherence Tomography for the Monitoring of Lesion Area Progression in Stargardt Disease. Invest Ophthalmol Vis Sci. 2016;57(9):OCT247-252.
71. Sodi A, Mucciolo DP, Cipollini F, et al. En face OCT in Stargardt disease. Graefes Arch Clin Exp Ophthalmol. 2016;254(9):1669-1679.
72. Greenstein VC, Nunez J, Lee W, et al. A Comparison of En Face Optical Coherence Tomography and Fundus Autofluorescence in Stargardt Disease. Invest Ophthalmol Vis Sci. 2017;58(12):5227-5236.
73. Alabduljalil T, Patel RC, Alqahtani AA, et al. Correlation of Outer Retinal Degeneration and Choriocapillaris Loss in Stargardt Disease Using En Face Optical Coherence Tomography and Optical Coherence Tomography Angiography. Am J Ophthalmol. 2019;202:79-90.
74. Georgiou M, Kane T, Tanna P, et al. Prospective Cohort Study of Childhood-Onset Stargardt Disease: Fundus Autofluorescence Imaging, Progression, Comparison with Adult-Onset Disease, and Disease Symmetry. Am J Ophthalmol. 2020;211:159-175.
75. Tanna P, Georgiou M, Strauss RW, et al. Cross-Sectional and Longitudinal Assessment of the Ellipsoid Zone in Childhood-Onset Stargardt Disease. Transl Vis Sci Technol. 2019;8(2):1.
76. Cideciyan AV, Aleman TS, Swider M, et al. Mutations in ABCA4 result in accumulation of lipofuscin before slowing of the retinoid cycle: A reappraisal of the human disease sequence. Hum Mol Genet. 2004;13(5):525-34.
77. Kayatz P, Thumann G, Luther TT, Jordan JF, Bartz-Schmidt KU, Esser PJ, Schraermeyer U. Oxidation causes melanin fluorescence. Invest Ophthalmol Vis Sci. 2001;42(1):241-6.
78. Cideciyan AV, Swider M, Aleman TS, et al. ABCA4-associated retinal degenerations spare structure and function of the human parapapillary retina. Invest Ophthalmol Vis Sci. 2005;46(12):4739-46.
79. Nassisi M, Mohand-Saïd S, Andrieu C, et al. Peripapillary Sparing With Near Infrared Autofluorescence Correlates With Electroretinographic Findings in Patients With Stargardt Disease. Invest Ophthalmol Vis Sci. 2019;60(15):4951-4957.
80. Burke TR, Rhee DW, Smith RT, et al. Quantification of peripapillary sparing and macular involvement in Stargardt disease (STGD1). Invest Ophthalmol Vis Sci. 2011;52(11):8006-15.
81. Curcio CA, Sloan KR, Kalina RE, et al. Human photoreceptor topography. J Comp Neurol. 1990;292(4):497-523.
82. Khan KN, Kasilian M, Mahroo OAR, et al. Early Patterns of Macular Degeneration in ABCA4-Associated Retinopathy. Ophthalmology. 2018;125(5):735-746.
83. Lee W, Nõupuu K, Oll M, et al. The external limiting membrane in early-onset Stargardt disease. Invest Ophthalmol Vis Sci. 2014;55(10):6139-49.
84. Wang X, Hoshi S, Liu R, Zhang Y. Modeling Human Macular Cone Photoreceptor Spatial Distribution. Invest Ophthalmol Vis Sci. 2024;65(8):14.
85. Mata NL, Radu RA, Clemmons SC, et al. Isomerization and oxidation of vitamin a in cone-dominant retinas: a novel pathway for visual-pigment regeneration in daylight. Neuron. 2002 ;36(1):69-80.
86. Ahmad KM, Klug K, Herr S, et al. Cell density ratios in a foveal patch in macaque retina. Vis Neurosci. 2003;20(2):189-209.
87. Long KO, Fisher SK, Fariss RN, et al. Disc shedding and autophagy in the cone-dominant ground squirrel retina. Exp Eye Res. 1986;43(2):193-205.
88. Strauss RW, Ho A, Muñoz B, et al. The Natural History of the Progression of Atrophy Secondary to Stargardt Disease (ProgStar) Studies: Design and Baseline Characteristics: ProgStar Report No. 1. Ophthalmology. 2016;123(4):817-28.
89. Kong X, West SK, Strauss RW, et al. Progression of Visual Acuity and Fundus Autofluorescence in Recent-Onset Stargardt Disease: ProgStar Study Report #4. Ophthalmol Retina. 2017;1(6):514-523.

Figure Legends

Fig. 1. Genetic prevalence of STGD1 (*ABCA4*-associated inherited retinal diseases) in various world populations. For the explanation of the underestimates and overestimates of prevalence figures, see Table 1 caption.

Fig. 2. Fluorescence properties of *Abca4*$^{-/-}$ RPE and retina explants. Figure is from Bui et al. [27]. A) Representative fluorescence emission spectra obtained from explants of RPE-choroid (dashed line) and retina (solid line) of an 8-month-old *Abca4*$^{-/-}$ eyecup are shown (excitation = 460 nm). This result was observed in three *Abca4*$^{-/-}$ mice of this age. B) Analysis of retina explants from *Abca4*$^{-/-}$ mice at 1, 4, and 8 months of age (n = 3 in each age group) revealed an age-dependent accumulation of the 625 nm-emitting fluorophore with 460 nm excitation. RFU, relative fluorescent units. The fluorescence spectrometer was optimally calibrated for each sample to account for differences in tissue depth and thickness.

Fig. 3. Identification of dominant fluorophores in *Abca4*$^{-/-}$ retinas. Figure is from Bui et al. [27]. Extracts were prepared from retinas of *Abca4*$^{-/-}$ mice aged 1, 4, and 8 months. The extracts were analyzed by HPLC using absorbance (500 nm) and fluorescence detection (excitation = 440 ± 20 nm, emission = 550 ± 20 nm). A) A representative chromatographic analysis of retinal extracts from a 1-month-old *Abca4*$^{-/-}$ mouse is shown. Absorbance and fluorescence emission chromatograms are shown as dashed and solid traces, respectively. The absorbance spectrum of peak eluting at ~6 minutes is shown; no fluorescence was associated with this peak. The absorbance and fluorescence emission spectra of the peak eluting at ~26 min are shown in the center and right panel insets, respectively. B) The emission intensity (peak height in light units [LU]) of the compound eluting at ~26 min increased in an age-dependent manner.

Fig. 4. Chromatographic analysis of extracts from human retina and RPE. Figure is from Mata et al. [24]. Panels A and D show analysis of retina and RPE, respectively, from a 71-year-old female with no retinal pathology as a representative control. Panels B and E show analysis of retina and RPE, respectively, from a 62-year-old female diagnosed with FFM. Panels C and F show analysis of retina and RPE, respectively, from a 73-year-old male diagnosed with STGD1. Chromatograms are shown at detection wavelengths of 500 (dark purple tracing) and 205 nm (green tracing) to detect absorbance by retinoid species and phospholipids, respectively. For panels A-C, the 205 nm absorbance scale is in absorbance units (AU), and for panels D-E, the 500 nm absorbance scale is in milliabsorbance units (mAU). Peaks corresponding to phosphatidylethanolamine (PE) in the retina samples are indicated with black arrows; peaks corresponding to A2PE-H2 are indicated with black arrows; peaks corresponding to A2E are indicated with blue arrows. The insets show absorption spectra for the identified A2PE-H2 and A2E peaks.

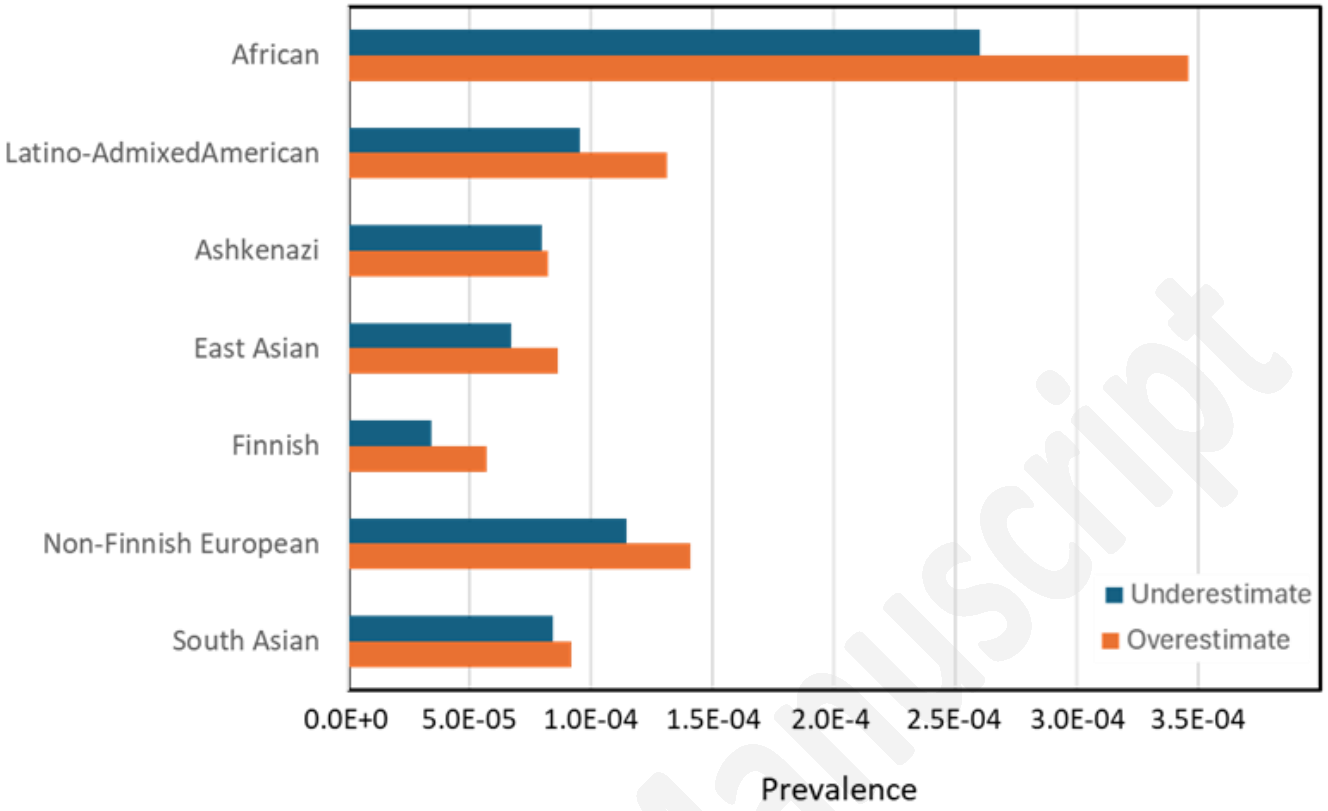

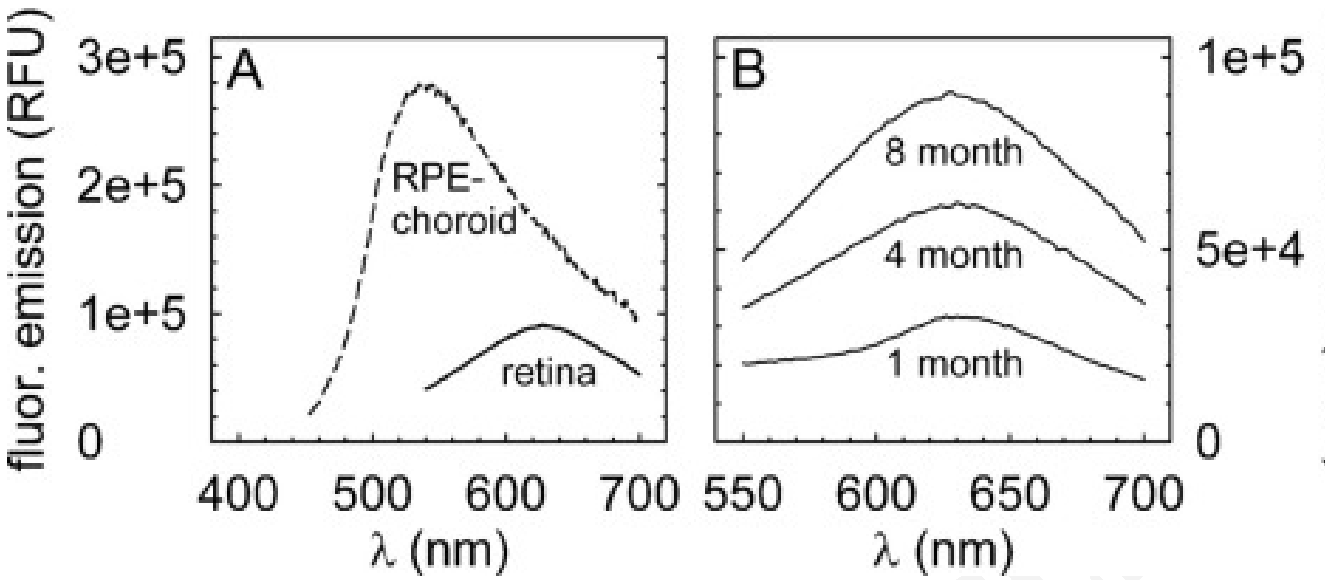

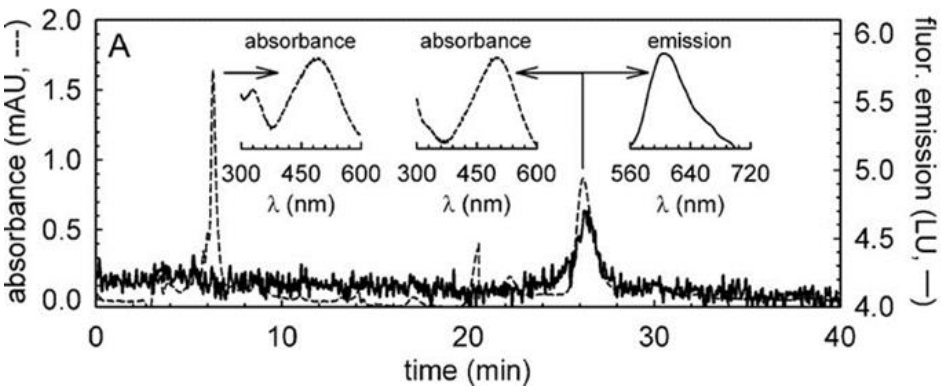

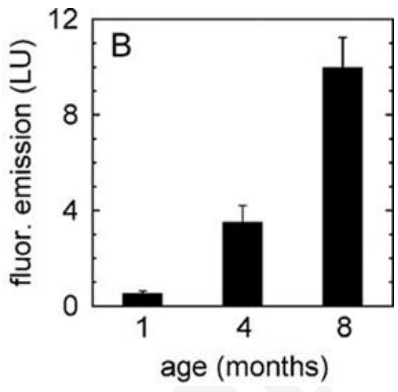

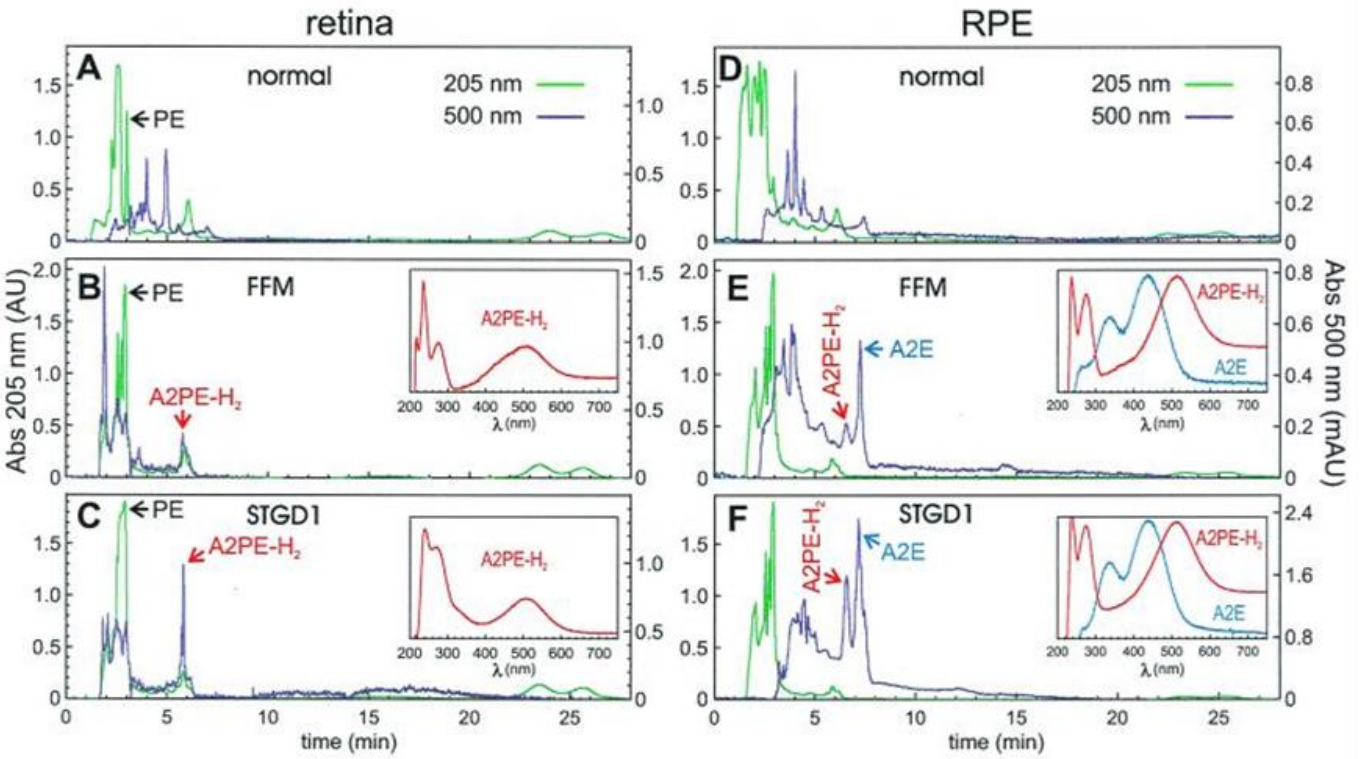

Table 1. Genetic prevalence of STGD1 (*ABCA4*-associated inherited retinal diseases) in various world populations based.

Both underestimates and overestimates are provided as per Cornelis et al. [22]. This is due to a subset of variants (n=192) that were inconclusively allocated to 2 severity categories. In the underestimate allele frequency populations, all ambiguous variants were allocated to the least severe category, while those same variants were allocated to the most severe category in the overestimate allele frequency populations.

Ethnicity	Prevalence Classic		Prevalence of Late-Onset*		Prevalence Total	
	Underestimate	Overestimate	Underestimate	Overestimate	Underestimate	Overestimate
African	1/3,846	1/2,891	1/475,783	1/357,046	1/3,815	1/2,868
Latino/Admixed American	1/10,458	1/7,623	1/330,964	1/271,922	1/10,138	1/7,415
Ashkenazi	1/12,516	1/12,132	1/668,003	1/668,997	1/12,286	1/11,916
East Asian	1/14,862	1/11,553	N/A	N/A	1/14,862	1/11,553
Finnish	1/29,030	1/17,579	1/326,737	1/323,645	1/26,661	1/16,686
Non-Finnish European	1/8,730	1/7,100	1/70,510	1/68,454	1/7,768	1/6,433
South Asian	1/11,885	1/10,875	1/338,536	1/321,727	1/11,482	1/10,519

*Adjusted for 5% penetrance of p.N1868I.

Table 2. Estimated patient population sizes of STGD1.

Region/Country	gnomAD Ethnicity	Population, n	Patients With STGD1, n (Based on Cornelis et al. [22])	
			Underestimate	Overestimate
Europe*	European	742,000,000	95,517	115,345
Australia*	European	26,640,000	3,429	4,141
China	East Asian	1,411,000,000	124,500,000	334,900,000
Japan	East Asian	124,500,000	8,377	10,777
United States	Mixed	334,900,000	46,767	59,235

*Non-Finnish population.

Table 3. United States subpopulations affected by STGD1.

Race	gnomAD Ethnicity	US Population, n	US Patients With STGD1, n (Based on Cornelis et al. [22])	
			Underestimate	Overestimate
White*	European	200,940,000	25,867	31,236
Latino	Latino-Admixed American	66,980,000	6,607	9,032
Black	African	50,235,000	13,166	17,517
Asian	East Asian	16,745,000	1,127	1,449

*Non-Finnish population.